ELSEVIER

BioSystems 58 (2000) 93–100

Bio Systems

www.elsevier.com/locate/biosystems

A pulse-type hardware neuron model with beating, bursting excitation and plateau potential

Yoshinobu Maeda [a,*], Hideo Makino [b]

[a] *Department of Biocybernetics, Faculty of Engineering, Niigata University, 8050 Ikarashi-2, Niigata 950-2181, Japan*
[b] *Department of Information Engineering, Faculty of Engineering, Niigata University, 8050 Ikarashi-2, Niigata 950-2181, Japan*

Abstract

We proposed a pulse-type hardware neuron model. It could reproduce simple excitations, beating and bursting discharges as well as an action potential with a plateau potential observed in living membranes. The model exhibited one of these dynamics depending on parameter values of the model's circuit. They include resistance, capacitance and externally injected DC current intensity. We studied the model's dynamics based on hardware experiments and mathematical analyses. Our results showed that two inward currents introduced into the model and differences in their operating time scales determined dynamics of the model. In particular, we illustrated a mechanism of the bursting discharges generation in terms of bifurcation theory and time-dependent changes in the form of instantaneous current–voltage characteristics of the model.

Keywords: Bifurcation; Hodgkin–Huxley equation; Excitable media; Current–voltage relationship

1. Introduction

Neuronal membranes generate brief electrical pulses, referred to as action potentials, spikes and firings as well. They are considered as the dominant information carrier in nervous systems. A typical excitable membrane generates an action potential in response to a brief electrical stimulation. It can also exhibit a regular train of action potentials (referred to as beating in this paper) in response to large enough DC current stimulation. A number of mathematical models of electrical excitations in living membranes have been proposed after Hodgkin–Huxley (HH) equation (Hodgkin and Huxley 1952). They include HH-type, i.e. channel-based, equations. The HH-type equations for bursting excitations can reproduce alternating dynamics between active state accompanied by several spikes and quiescent state without them (Rinzel and Lee 1986; Chay and Cook 1988; Hayashi and Ishizuka 1992; Rush and Rinzel 1994; Fan and Chay 1994; Guckenheimer et al. 1997). Some HH-type equations can generate an action potential with a plateau potential common in cardiac Purkinje fiber cell (Noble 1966). Most of these models were constructed only by introducing extra-ionic channels (currents) and by adding corresponding terms to the original HH equation. Successful reproductions of

* Corresponding author. Tel.: +81-25-2627776.
E-mail address: maeda@bc.niigata-u.ac.jp (Y. Maeda).

0303-2647/00/$ - see front matter
PII: S0303-2647(00)00111-8

these diverse types of action potential generation by HH-type equations may be due to simple and physiologically plausible formulation of the equations.

Recently, modeling of membrane dynamics has begun to attract researches in the field of nonlinear dynamical system theory. For instance, systematic changes in an appropriate physiological parameter value, such as externally injected current intensity, results in qualitative and abrupt changes in the living membrane dynamics. Such changes may be described by the bifurcation theory. Indeed, plausibility of recent proposed HH-type membrane models is evaluated not only by reproducibility of action potential waveforms at single fixed physiological parameter value but also by that at various parameter values (Chay and Cook 1988; Hayashi and Ishizuka 1992; Rush and Rinzel 1994; Fan and Chay 1994). In other words, a membrane model should be embedded appropriately in the model's parameter space so that it can reproduce a sequence of bifurcations exhibited by the real neuronal membrane as a function of physiological parameter values.

Our main interest of the present study is to construct a pulse-type hardware neuron (HN) model that can reproduce bursting discharges of action potentials emerging through a sequence of bifurcations. We use the term 'pulse-type' to distinguish the models from conventional threshold devices as artificial neuron-like elements. Why 'hardware' models? There are several advantages to study HN models instead of purely mathematical equations. (1) A HN model can provide real time processing. Thus it may be suited for studying a large-scale neural network dynamics when many HN models are connected with each other; (2) Physical interpretation of each parameter of a model is quite obvious, and, in some cases, it is easily associated with electro-physiological quantities of membranes; (3) Circuit dynamics can be described by a mathematical equation. Thus, one can achieve both circuit experiments and mathematical analyses for better understanding of the dynamics. Several pulse-type bursting HN models have been constructed under motivations similar to ours (Gulrajani et al. 1977; Sekine et al. 1999). To our knowledge, however, pulse-type HN models that can reproduce bursting discharges emerging through an appropriate sequence of bifurcations (i.e. observed in physiological experiments) have not been reported.

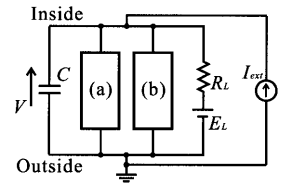

Fig. 1. A model of an excitable membrane. The branches (a) and (b) correspond to the sodium and potassium ionic channels, respectively.

2. Pulse-type hardware neuron model

Many pulse-type HN models of excitable membranes have been constructed (Harmon 1961; Murai et al. 1977; Gulrajani et al. 1977; Hoshimiya et al. 1979; Keener 1983; Sekine et al. 1999). Fig. 1 illustrates the model proposed by Hoshimiya et al. It has four branches as in the electrical equivalent circuit of HH equation. V, C, R_L, E_L and I_{ext} represent the membrane potential, membrane capacitance, leakage resistance, leakage Nernst equilibrium potential and the injected DC current input, respectively. The branches (a) and (b) correspond to the V-dependent inward sodium and the delayed outward potassium ionic channels of HH equation, respectively. They are detailed in Fig. 2. Each of them consists of two units, that is, the ionic current part and the parallel-connected conductance-control part. The latter is marked by the dotted square. E_{Na} and E_K correspond to

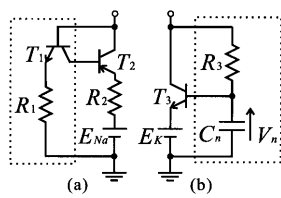

Fig. 2. Circuit descriptions. (a) and (b) details the branches (a) and (b) of Fig. 1, respectively. The circuits marked by the dotted squares represent the activation units of the sodium and potassium current, respectively.

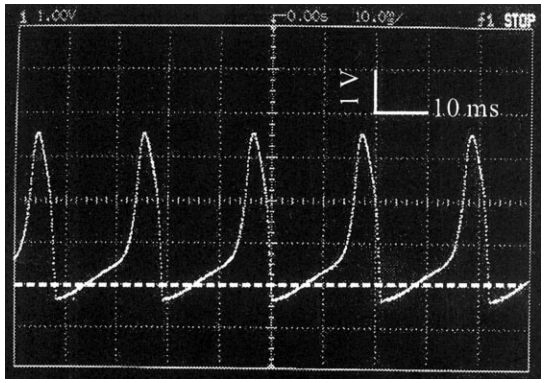

Fig. 3. Typical dynamics in the hardware neuron model of Fig. 1. The parameters are $C = 0.5$ μF, $C_n = 1.0$ μF, $R_L = 100$ kΩ, $R_1 = 200$ kΩ, $R_2 = 2$ kΩ, $R_3 = 100$ kΩ, $E_{Na} = 5$ V, $E_K = -0.4$ V, $E_L = 0$ V, $T_1 = T_3$: npn-type 2SC1815, T_2: pnp-type 2SA1015, and $I_{ext} = 0.1$ mA. The ordinate is the membrane potential V.

sodium and potassium Nernst equilibrium potentials in HH, respectively. A cut-in voltage of the transistor T_1 acts as the excitation threshold. The sodium ionic current I_{Na} is switched on when the membrane potential V exceeds it. The potassium ionic current I_K is switched on when V_n in the figure exceeds the cut-in voltage of the transistor T_3. In this HN model, the gating variables m and h of HH equation are not considered. Therefore, the dynamics of the HN model can be described by differential equations with two variables, V and V_n. Thus, the HN model is regarded as a reduced version of HH equation (FitzHugh 1961; Nagumo et al. 1962; Rinzel 1985; Kepler et al. 1992).

When the values of the resistors, the capacitors and the voltage sources are set so that the resting potential is equal to the potassium Nernst equilibrium potential $E_K (\leq 0)$, this HN model shows periodic beating discharges for an appropriate DC current injection (Fig. 3). The mechanisms of action potential generation in this model are briefly described as follows: (i) I_{ext} charges up C until V exceeds the cut-in voltage of T_1; (ii) T_1 is turned on; (iii) T_2 is also turned on; (iv) I_{Na} that released from the source of E_{Na} to the inside of the membrane charges up C, and as the result, V becomes more positive toward E_{Na} (action potential generation); (v) I_{Na} charges up C_n slower than C; (vi) V_n shifts upward until it exceeds the cut-in voltage of T_3; (vii) T_3 is turned on; (viii) V rapidly shifts downward by I_K from *Collector* to *Emitter* of T_3. As the result, V varies suddenly down toward E_K.

When periodic pulse trains are applied to this model, the HN model shows either phase-locked or chaotic responses (Yamawaki et al., 1995). The firing frequency of the phase-locked response takes the form of an extended Cantor function. The chaotic response appears between the phase-locked responses. As such, it can show qualitatively the same responses as those observed in the squid giant axon (Takahashi et al., 1990) and the FitzHugh–Nagumo (FHN) equation (Sato and Doi, 1992).

In the next section, we construct a bursting HN model by modifying this HN model. It can even show plateau potentials. We set $R_2 = 0$ and $E_K = E_L = 0$ throughout the paper for simplicity.

3. Bursting hardware neuron model

Differential equation models of bursting discharges can be classified into several types such as square-wave, parabolic and elliptic bursters (Rinzel and Lee 1986; Bertram et al. 1995; Guckenheimer et al. 1997; Hoppensteadt and Izhikevich 1997; De Vries and Miura 1998). The square-wave bursters show firings on plateau potentials, and they should be described by at least three variables (Chay and Cook 1988; Fan and Chay 1994; Av-Ron 1995; Maeda et al. 1998). One of the three variables is associated with an excitation with fast dynamics (fast variable or fast system) responsible for the depolarization of the plateau and action potentials. The second is a refractoriness of the fast variable (refractory fast system) responsible for the repolarization of the action potentials during each active state. The other is a refractory slow variable (slow system) responsible for the repolarization of the plateau potential, and its activation terminates the active state.

We propose a bursting HN model as shown in Fig. 4. The model's dynamics can be described by three-dimensional differential equations. In com-

parison this bursting HN model with the simple excitable HN model shown in Fig. 1, the most important difference is that the former has two branches (b) and (b') associated with active outward currents, while the latter has only one branch (b). The branch (b) of the bursting HN model corresponds to the refractory slow system. The branch (b') represents the refractory fast system. It is a modification of (b) in Fig. 4, i.e. a transistor T_4 is added. T_4 completely rectifies the outward current of the branch (b'), since both *Base-Emitter* and *Base-Collector* units are located in reverse directions against the inward current. Therefore, the capacitor C_n cannot discharge through T_4. So, when T_3 is turned off, V_n remains constant, leading to the plateau potential. As the result, the excitable and the refractory fast systems are able to regenerate the action potentials until the refractory slow system repolarizes the plateau potential. We obtained a typical bursting by choosing the capacitor and resistor values as follows: $C = 1/3$, $C_n = 0.5$, $C_s = 1.0$ in μF, and $R_L = 100$, $R_1 = 200$, $R_s = 100$ in kΩ, and $E_{Na} = 5$ in V.

In our circuit experiment, we changed the two parameters I_{ext} and R_n systematically as the bifurcation parameters. First, we investigated influences of I_{ext} on behavior with R_n fixed to $R_s/10$, and then those of R_n for a fixed I_{ext}. We expected, from the roles of each parameter, that the former would be associated with the modification of firing patterns such as beatings and burstings, and the latter with the generation of the plateau potential.

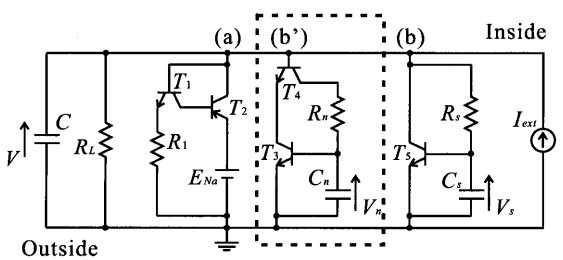

Fig. 4. A bursting hardware neuron model. The branches (a), (b') and (b) correspond to the inward, fast and slow outward ionic channels, respectively.

4. Results

4.1. I_{ext}-dependent dynamics

For $I_{ext} > 2.15$ mA, V was at the quiescent state. As the value of I_{ext} decreased, beatings, periodic and chaotic burstings were observed in this order. For $I_{ext} < 0.002$ mA, V was at the quiescent state again. Fig. 5 (a to f) shows the temporal waveforms of V in their stationary states as typical dynamics of the bursting HN model. Those include, (a) beating; (b) periodic bursting with two spikes in one active state; (c) periodic bursting with two different active states with two spikes within each; (d) chaotic bursting; (e) periodic bursting with three spikes in one active state; and finally (f) periodic bursting with six spikes in one active state. The changes from (a) to (d), i.e. from the beating to the periodic bursting with three spikes, formed a cascade of the period-doubling bifurcations. We refer to the increase in the number of spikes during one active state from (d) to (f) as a 'period-adding'.

4.2. R_n-dependent dynamics

We summarize the R_n-dependent changes in the dynamics of the model. Here, I_{ext} was fixed at 0.01 mA. As R_n decreased, amplitudes of the action potentials during the active states became smaller. A typical behavior is exemplified in Fig. 6(a) ($R_n = 8$ kΩ). As R_n decreased further, only one action potential was observed at the beginning of each active state. Fig. 6(b) ($R_n = 5$ kΩ) shows this behavior. The temporal waveform with the plateau potential was similar to that observed in the cardiac Purkinje fibers.

4.3. Generating mechanism of bursting discharge

In order to clarify the mechanism of bursting generations, we investigated instantaneous current-voltage relations $i_{inst} = i_{inst}(V)$ of the bursting HN model. Fig. 7(a–f) illustrates time-dependent changes in the shape of i_{inst}-V curve at appropriate instants during the bursting. For some instants, there were two negative resistance regions (for example, Fig. 7(b) and (d)) and five roots on

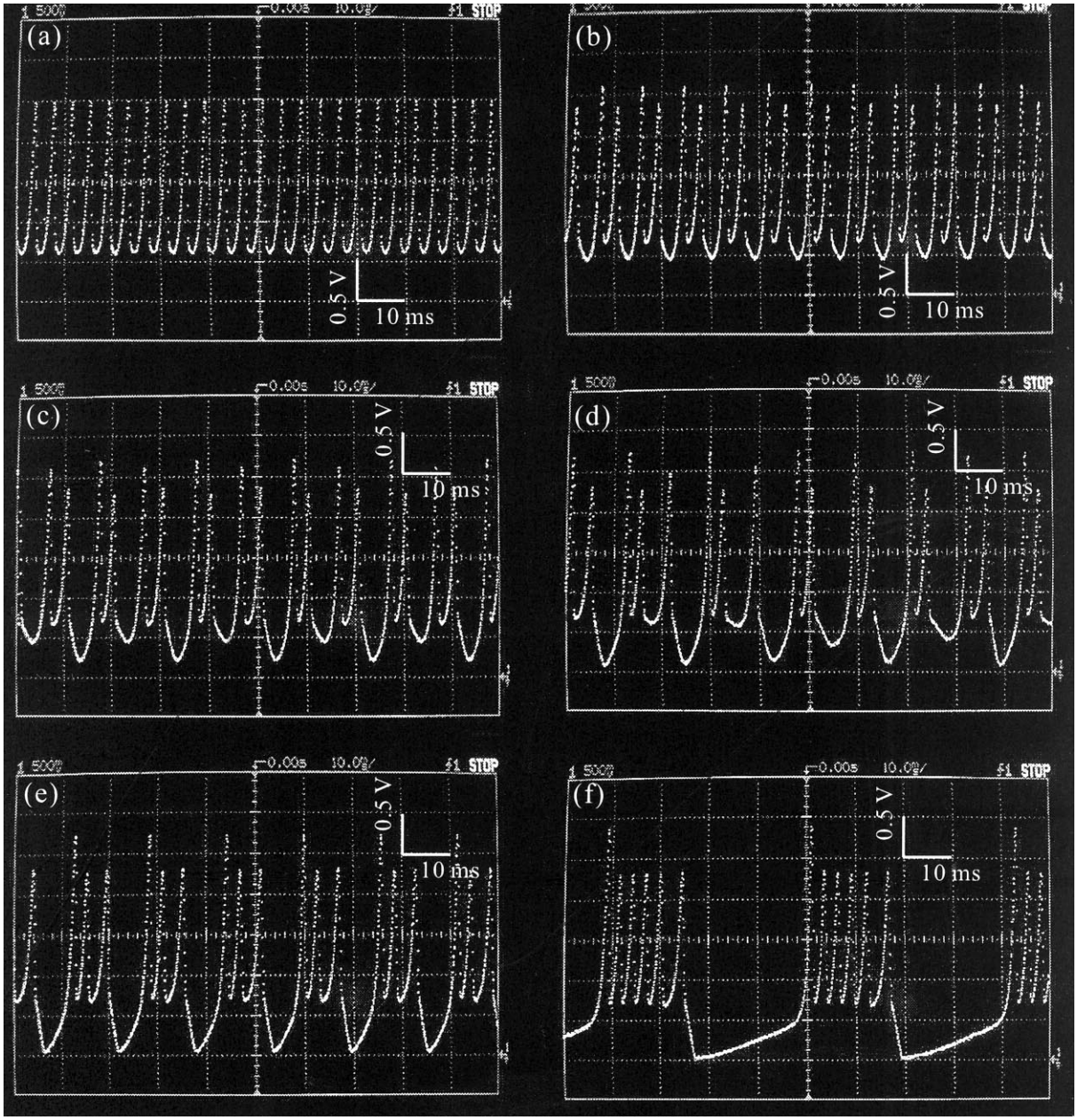

Fig. 5. Typical dynamics of the bursting hardware neuron model. The parameters are $R_n = 10$ kΩ, $T_1 = T_3 = T_4 = T_5$: npn-type 2SC1815, T_2: pnp-type 2SA1015. I_{ext} is set to (a) 0.7, (b) 0.6, (c) 0.45, (d) 0.30, (e) 0.2 (f) 0.01 in mA, respectively. The ordinates are the membrane potential V.

the horizontal axis ($i_{\text{inst}}(V) = 0$), as indicated by the symbols R, ET1, P, ET2, and M. These voltages were associated with the resting potential, the excitation threshold for plateau potential onset, the plateau potential, the excitation threshold for the action potential onset and the maximum value of the action potential, respectively.

When the state point was at the point *R*, the DC current input brought the membrane potential (the state point) toward the excitation threshold ET1. Then the state point started to move to the point M (Fig. 7(a)). The depolarization of the membrane potential shifted the i_{inst}-V curve between ET1 and M upward, and P and ET2 appeared (Fig. 7(b)). This change was associated with increases of the delayed outward current generated by the refractory fast system (branch (b') in the circuit). As the outward current increased, the right side negative resistance portion was shifted upward. It caused that the point M collided with ET2, and they vanished. Then the state point rapidly moved back to the point P (Fig. 7(c)). This repolarization of the membrane potential induced the downward shift of the curve, since the inward current generated by the excitable fast system (branch (a) in the circuit) increased again. Then ET2 and M appeared again (Fig. 7(d)), before P collides with ET2. The state point rapidly moved to the point M again (Fig. 7(e)), after P and ET2 vanished. This process from Fig. 7(b) to (e) repeated several times depending on the number of the spikes within one active state. During the active state, the refractory slow system (branch (b) in the circuit) was activated gradually. The outward current generated by the refractory slow system caused the upward shift of the curve between *R* and *P*. Eventually the point P collides with ET1, and they vanished. As the result, the state point moved back to the point *R* (Fig. 7(f)), referred to as the quiescent state.

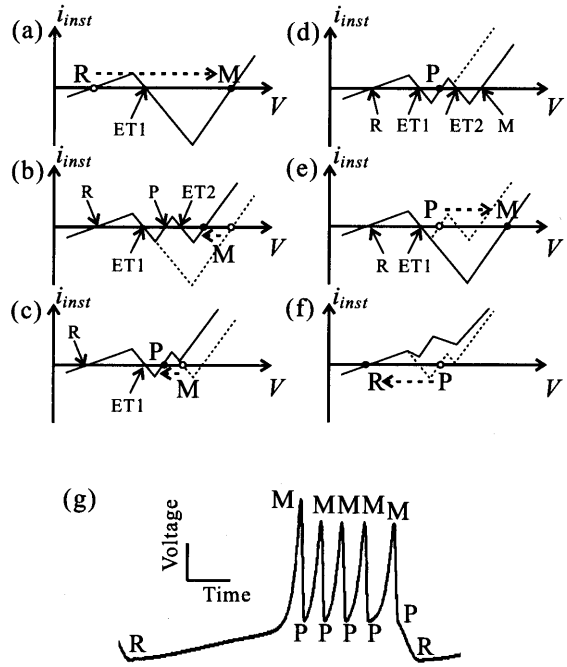

Fig. 7. Mechanism of bursting discharge generations. (a)–(f) Schematic diagrams of the time-dependent changes in the instantaneous current–voltage curve of the bursting HN model. Three stable points *R*, *P* and *M* correspond to the resting, the plateau and the maximum peak potential, respectively. Two unstable points ET1 and ET2 are excitation thresholds, respectively. Abscissas are the voltage and ordinates are the outward current. (g) Qualitative corresponding points of *R*, *P* and *M* to the temporal waveform

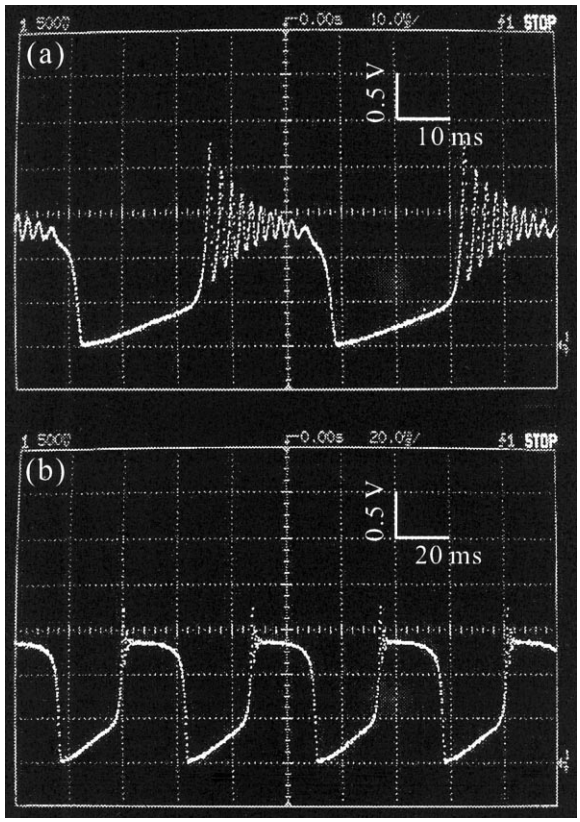

Fig. 6. Stationary temporal waveforms with the plateau potentials. The parameters are $I_{ext} = 0.01$ mA, $T_1 = T_3 = T_4 = T_5$: npn-type 2SC1815. R_n is set to (a) 8 kΩ, (b) 5 kΩ.

5. Discussion

We constructed a bursting hardware neuron (HN) model, and analyzed its dynamics and bifurcations. We obtained a sequence of bifurcations in the model. These were the period-doubling from beating to bursting and the period adding cascade as I_{ext} changed. Such similar bifurcations have been observed in the physiological experiment in bursting cells. They have been also observed in many pulse-type mathematical models (e.g. Hayashi and Ishizuka 1992; Fan and Chay 1994). Thus, one can consider that these are universal features of bursting neurons and their models. As R_n changed, the HN model showed the action potentials with the plateau potential.

We show that each of the five branches of our two-terminal electronic circuit model can be interpreted physiologically based on the corresponding ionic channels. Although we did not describe the result in this short paper, we confirmed that the temporal waveform of the equivalent potential V_s was similar to those of the slow dynamics of the intracellular calcium concentration of the pancreatic β-cell model with two outward currents (the delayed and the Ca-dependent potassium ionic channels) (Fan and Chay 1994; Av-Ron 1995). In this sense, the branches (b') and (b) of Fig. 4 can be interpreted as the delayed V-dependent and the Ca-dependent potassium ionic channels, respectively. The original HH equations can also show the plateau potentials when the dynamics of the potassium activation variable n is set slower than the sodium inactivation variable h (Doi and Kumagai 1999). In this sense, the branch (b') of Fig. 4 could be also reinterpreted as the inactivation system of the sodium ionic channel, though we regarded it as the delayed potassium ionic channel. It is possible to accept these two interpretations based on the fact that the activation of the potassium ionic channel and the inactivation of the sodium ionic channel synergistically cause the outward current.

We showed that our HN model could reproduce relatively rich nonlinear dynamics ranging from beating to bursting dynamics. Nevertheless, our model consisted of just five transistors, four resistors, three capacitors and one voltage source, so that it could be treated as a minimal bursting hardware neuron model. One can easily implement our model into an analog circuit, and utilize it as one of the components of realistic artificial neural networks. It is our future subject to construct a network of our HN models and to investigate how its dynamics changes as a function of dynamics of each HN model.

Acknowledgements

The authors would like to thank Professor Shunsuke Sato and Professor Donald Nicholson Parkes for their helpful discussions. YM thanks Professor Oscar Diez Martinez for reading our manuscript and for valuable comments.

References

Av-Ron, E., 1995. Modeling a small neural network: the lobster cardiac ganglion. J. Biol. Sys. 3, 4, 1087–1104.

Bertram, R., Butte, M.J., Kiemel, T., Sherman, A., 1995. Topological and phenomenological classification of bursting oscillations. Bull. Math. Biol. 57, 413–439.

Chay, T.R., Cook, D.L., 1988. Endogenous bursting patterns in excitable cells. Math. Biosci. 90, 139–153.

De Vries, G., Miura, R.M., 1998. Analysis of a class of models of bursting electrical activity in pancreatic β-cells. SIAM J. Appl. Math. 58, 607–635.

Doi, S., Kumagai, S., 1999. Rich nonlinear dynamics of HH-type neurons with multiple time scales. The 3rd Int. Workshop on Neuronal Coding, 117–120.

Fan, Y.S., Chay, T.R., 1994. Generation of periodic and chaotic bursting in an excitable cell model. Biol. Cybern. 71, 417–431.

FitzHugh, R., 1961. Impulses and physiological states in theoretical models of nerve membrane. Biophys. J. 1, 445–466.

Guckenheimer, J., Harris-Warrick, B., Peck, J., Willms, A., 1997. Bifurcation, bursting, and spike frequency adaptation. J. Comp. Neurosci. 4, 257–277.

Gulrajani, R.M., Roberge, F.A., Mathieu, P.A., 1977. The modelling of a burst-generating neuron with a field-effect transistor analog. Biol. Cybern. 25, 227–240.

Harmon, L.D., 1961. Studies with artificial neurons, I: Properties and functions of an artificial neuron. Kybernetik 1, 89–101.

Hayashi, H., Ishizuka, S., 1992. Chaotic nature of bursting discharge in the *Onchidium* pacemaker neuron. J. Theor. Biol. 156, 269–291.

Hodgkin, A.L., Huxley, A.F., 1952. A quantitative description of membrane current and its application to conduction and excitation in nerve. J. Physiol. 117, 504–544.

Hoppensteadt, F.C., Izhikevich, E.M., 1997. Weakly Connected Neural Networks. Springer.

Hoshimiya, N., Yoshida, S., Shogen, K., Matsuo, T., 1979. Two-terminal electronic circuit neuron model with excitable membrane V-I-t characteristics. Biol. Cybern. 35, 125–130.

Keener, J.P., 1983. Analog circuitry for the van der Pol and FitzHugh-Nagumo equations. IEEE Trans., SMC-13 5, 1010–1014.

Kepler, T.B., Abbott, L.F., Marder, E., 1992. Reduction of conductance-based neuron models. Biol. Cybern. 66, 381–387.

Maeda, Y., Pakdaman, K., Nomura, T., Doi, S., Sato, S., 1998. Reduction of a model for an *Onchidium* pacemaker neuron. Biol. Cybern. 78, 265–276.

Murai, T., Yagi, H., Yotuya, H., 1977. Electronical excitable membrane model with time variant negative resistance. Technical Report of IEICE, MBE77-6, 19–24 (in Japanese).

Nagumo, J., Arimoto, J., Yoshizawa, S., 1962. An active pulse transmission line stimulating nerve axon. Proc IRE 50, 2061–2070.

Noble, D., 1966. Applications of Hodgkin-Huxley equations to excitable tissue. Phys. Rev. 46 (1), 1–50.

Rinzel, J., 1985. Excitation dynamics: insights from simplified membrane models. Fed. Proc. 44, 2944–2946.

Rinzel, J., Lee, Y.S., 1986. On different mechanisms for membrane potential bursting. In: Othmer, H.G. (Ed.), Lecture Notes in Biomathematics. Springer, pp. 19–33.

Rush, M.E., Rinzel, J., 1994. Analysis of bursting in a thalamic neuron model. Biol. Cybern. 71, 281–291.

Sato, S., Doi, S., 1992. Response characteristics of the BVP neuron model to periodic stimuli. Math. Biosci. 112, 243–259.

Sekine, Y., Someya, K., Saeki, K., Aihara, K., 1999. A study on neuronal coding using pulse-type hardware chaotic neuron model. The 3rd Int. Workshop on Neuronal Coding, 121–124.

Takahashi, N., Hanyu, Y., Musha, T., Kubo, R., Matsumoto, G., 1990. Global bifurcation structure in periodically stimulated giant axons of squid. Physica D 43, 318–334.

Yamawaki, N., Sato, S., Doi, S., 1995, Effect of the stimulus pulse width upon the stimuli-response characteristics of an electronic excitable membrane model. Trans, IEE of Japan, 115-C, 1541-1547 (in Japanese).